BIOCHEMISTRY
including biophysical chemistry & molecular biology

Article

pubs.acs.org/biochemistry

Chimeric hERG Channels Containing a Tetramerization Domain are Functional and Stable

Georg J. Hausammann and Markus G. Grütter*

From the Department of Biochemistry, University of Zürich, Winterthurerstrasse 190, 8057 Zürich, Switzerland

Supporting Information

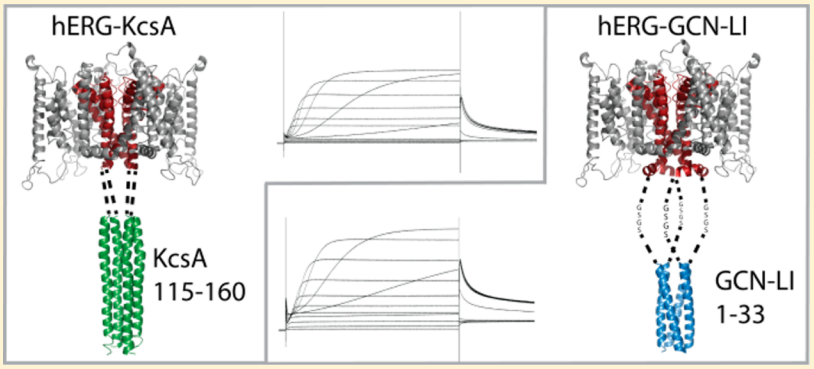

ABSTRACT: Biochemical and detailed structural information of human *ether-a-go-go-related gene* (hERG) potassium channels are scarce but are a prerequisite to understand the unwanted interactions of hERG with drugs and the effect of mutations that lead to long QT syndrome. Despite the huge interest in hERG, to our knowledge, procedures that provide a purified, functional, and tetrameric hERG channel are not available. Here, we describe hybrid hERG molecules, termed chimeric hERG channels, in which the N-terminal Per-Arnt-Sim (PAS) domain is deleted and the C-terminal C-linker as well as the cyclic nucleotide binding domain (CNBD) portion is replaced by an artificial tetramerization domain. These chimeric hERG channels can be overexpressed in HEK cells, solubilized in detergent, and purified as tetramers. When expressed in *Xenopus laevis* oocytes, the chimeric channels exhibit efficient trafficking to the cell surface, whereas a hERG construct lacking the PAS and C-linker/CNBD domains is retained in the cytoplasm. The chimeric hERG channels retain essential hERG functions such as voltage-dependent gating and inhibition by astemizole and the scorpion toxin BeKm-1. The chimeric channels are thus powerful tools for helping to understand the contribution of the cytoplasmic hERG domains to the gating process and are suitable for in vitro biochemical and structural studies.

The human *ether-a-go-go-related gene* (hERG) encodes a voltage-gated potassium channel that is mainly expressed in the heart and neural tissues as well as in certain tumor cell types.[1−3] In the heart, hERG is the main component of the delayed rectifier current I_{Kr}[4] that repolarizes the cardiac action potential. In tumor cells, it was shown that hERG modulates cell proliferation and apoptosis.[5]

Loss of hERG function, either through mutations in the *HERG* gene or through drug interactions, can cause inherited or acquired long QT syndrome (LQTS), respectively, provoke cardiac arrhythmias, and lead to sudden death.[6−9]

Inherited LQTS is caused by mutations in *HERG* that reduce I_{Kr} either by disruption of its synthesis, folding, trafficking, gating, or ion permeation. Impaired trafficking, the most common phenotype, results in retention of the mutated proteins in the ER and induction of chaperone expression.[10−12]

hERG shares the typical architecture of a voltage-gated channel with a voltage sensor comprising transmembrane helices S1 to S4 and a pore domain with the pore loop, S5 and S6.[13] This membrane part is flanked by the cytoplasmic Per-Arnt-Sim (PAS) domain at the amino terminus and the C-linker/cyclic nucleotide binding domain (CNBD) following the S6 helix. A critical residue for drug binding in acquired LQTS, F656, is located in the S6 helix of the channel. In the tetrameric channel, these residues point toward the water-filled pore and form a hydrophobic ring.[14]

The unusual gating of hERG is characterized by a slow activation and a fast inactivation process. The kinetic behavior is governed by the interplay of the cytoplasmic domains. Constructs with deletions of the PAS domain and the proximal N-terminus were reported to retain the hERG-like gating and to display a faster deactivation rate.[15] The PAS domain slows deactivation through interactions with the CNBD and the S4/S5 linker. The CNBD, however, delays the activation process, as a deletion of this domain decreases the time to reach half-maximal activation.[16,17]

Received: August 13, 2013
Revised: November 27, 2013
Published: November 28, 2013

dx.doi.org/10.1021/bi401100a | *Biochemistry* 2013, 52, 9237−9245

The C-linker/CNBD as well as the coiled-coil domain at the extreme C-terminus[17−19] are believed to contribute to the tetrameric channel assembly. Then again, the oligomeric state of the C-linker/CNBD domain in the recent crystal structures of related homologous potassium channels was monomeric for the ERG channel from mosquito (*Anopheles gambiae*) and dimeric for the ELK channel from zebrafish (*Danio rerio*).[20,21]

To date, there is no report on the overexpression of functional tetrameric hERG channels. This could be due to both low detergent solubility and weak oligomeric stability of hERG. Here, we promote the tetrameric interactions by replacing the hERG tetramerization domains with more stable heterologous tetrameric coiled-coil domains.

A similar approach was chosen by Kupfershmidt et al. They partially rescued the channel function of a construct with a deleted C-linker/CNBD by adding a coiled coil from the distal hERG C-terminus.[19]

To render the protein accessible to structural and biophysical studies while retaining the channel functions, we fused two types of tetramerization domains to the C-terminus of hERGΔNΔC: the cytoplasmic C-terminal KcsA helix and the GCN4-LI leucine zipper. Molina et al. reported that the deletion of the C-terminal KcsA-helix resulted in decreased tetrameric assembly and stability of the KcsA channel.[22] Therefore, we identified this helix as a suitable tetramerization domain for hERG. GCN-4-LI forms an extremely thermostable tetrameric parallel coiled coil. This 33-residue peptide was used to replace the inherent tetramerization domain, T1, of the Shaker potassium channel.[23] The oligomeric state of GCN4 is dictated by the aliphatic amino acids in positions a and d of the heptad repeat. With Leu and Ile it forms a tetramer, with Ile and Ile, a trimer, with Ile and Leu, a dimer, and with Asp and Asp, a monomer.[23,24]

To ensure the optimal orientation of the tetramerization domains relative to the pore, we chose two different linkers between GCN4-LI and hERGΔNΔC for the chimeric hERG-GCN-LI channel. For hERG-KcsA, a linker was omitted, but different KcsA start positions were selected.

We recorded the currents of the chimeric channels with two-electrode voltage-clamp, investigated their trafficking in oocytes, and analyzed the oligomerization of the purified proteins expressed in HEK cells by size-exclusion chromatography (SEC).

The channel function of an inactive, minimal hERG construct hERGΔNΔC could be restored by grafting a tetrameric coiled-coil domain onto its carboxy-terminus. The voltage-dependent gating activity measured with two-electrode voltage-clamp correlated well with the tetrameric state of the purified protein determined by SEC.

EXPERIMENTAL PROCEDURES

Molecular Biology. The synthetic Kv11.1 gene (UniProt: Q12809-1) with an optimized sequence was ordered from GenScript. The full-length protein and its truncations were amplified with primers containing SapI sites and cloned into a modified pInitial Vector for FX cloning.[25] The constructs in this vector were sequenced and then subcloned into a target vector modified for FX cloning: either into pTLN FX vector[26] for expression of its RNA in *Xenopus laevis* oocytes or a pcDNA 3.1 FX vector for expression in tsA201 HEK cells containing a HRV 3C protease-cleavage site, a Myc tag, and a SBP (streptavidin binding peptide) tag at the 3′ end of the construct.[27]

Various truncations of the full-length hERG protein were screened in tsA201 cells for their expression and solubility. The most important ones were 1−1159 (full length), 362−870 (hERGΔC), and 362−669 (hERGΔNΔC).

hERG Homology Model. To find a structural homologue of the hERG membrane part, we performed structure prediction using the server Phyre (protein homology/analogy recognition engine) implementing the hERG sequence from residues 365 to 670.[28] Phyre predicted hERG to be the structural homologue of the transmembrane region of a cyclic-nucleotide-regulated channel from *Mesorhizobium loti* (with 17% of identity), and the server could model hERG from residues 409 to 668.

Phyre predicted the C-linker/CNBD part of the hERG channel (residues 668−870) to resemble the CNBD structure of the HCN pacemaker channel. The server was able to model the CNBD domain from residues 669 to 861.

Both structures were then manually assembled using the program Coot and minimized using Phenix. A partial model was obtained spanning hERG residues 409−861.

Construction of Chimeric Channels. The underlined sequences of hERG 362−870 (L666YSGTARYHTQMLR679) in the pInitial vector were mutated using QuikChange site-directed mutagenesis to BspEI cleavage sites (encoding the SG dipeptide) and digested with BspEI and SapI.

The KcsA C-terminal cytoplasmic helix was amplified with a forward primer containing a 5′ BspEI cleavage site followed by a region annealing to KcsA (ordered from Mr. Gene) starting at position 115 and a SapI-containing reverse primer annealing at position 160. Further shorter KcsA helices were amplified with a different forward primer starting at positions 116, 117, and 118 and digested with BspEI and SapI.

The digested hERG fragment ending at position 669 was ligated with KcsA fragments with start positions ranging from 115 to 119 and then ligated into the SapI-cleaved pInitial vector. The resulting chimeric channels were hERG-KcsA 115, hERG-KcsA 116, hERG-KcsA 117, and hERG-KcsA 118.

The amino acid sequence of the GCN4-LI peptide from the N- to the C-terminus reads RMKQI^{d}EDKL^{a}EEI^{d}LSKL^{a}YHI^{d}ENEL^{a}ARI^{d}KKLL^{a}GER.

The trimeric GCN-4 II, dimeric GCN4-IL, and monomeric GCN-4 DD were constructed by QuikChange site-directed mutagenesis of the residues with superscripts in the GCN4-LI peptide. These residues occupy the positions a and d in the heptad repeat of the helical wheel. For GCN4-II, positions a and d were mutated to I and for GCN-IL, they were mutated to I and L. The monomeric version was constructed by replacing the two d positions in the center with D: RMKQI^{d}EDKL^{a}EED^{d}LSKL^{a}YHD^{d}ENEL^{a}ARI^{d}KKLL^{a}GER.[23,24]

The GCN-4 LI leucine zipper (ordered from Mr. Gene) was amplified with a forward primer containing a 5′ BspEI cleavage site followed by GS or GSGS linker and the complementary region and a SapI-containing reverse primer. The PCR product was digested with BspEI and SapI. The digested hERG part ending at position 676 was ligated with different GCN-4 fragments, -LI, -II, -IL, and -DD, and then ligated into the SapI-cleaved pInitial vector. These chimeric channels were named 75-gsgsLI, 75-gsgsII, 75-gsgsIL, and 75-gsgsDD.

The sequenced constructs in pInitial were cloned into the corresponding FX target vectors: pTLN FX and pcDNA-SBP FX.[27]

Transient Transfection. The tsA201 HEK cells were grown in DMEM containing 10% fetal bovine serum, penicillin

(100 u/ml), and streptomycin (100 μg/mL) (Sigma) in an atmosphere of 5% CO_2. Constructs in pcDNA-SBP FX (pcDNA 3.1 vector with a C-terminal 3c-Myc-SBP tag) were transiently transfected into tsA201 HEK cells using a modified calcium phosphate transfection method[29] and maintained at 2.8% CO_2. After 48 h, the cells were harvested by detaching, washed once in PBS, and frozen at −80 °C. GnTI$^-$ cells were transfected identically but grown in DMEM F12 Ham (Sigma) media with 10% fetal bovine serum, penicillin (100 u/ml), and streptomycin (100 μg/mL).

Purification. All purification steps were performed at 4 °C. For each construct, cells from a 200 mL expression volume were purified. Cells corresponding to one 10 cm petri dish were resuspended in 400 μL of lysis buffer (in mM): 50 Na_2HPO_4, pH 7.5, 290 NaCl, 10 KCl, 5 EDTA, Complete (Roche), and PMSF. To solubilize the membrane proteins, *n*-dodecyl-β-D-maltopyranoside (DDM, Anatrace) was added to 2% and incubated at 4 °C on a horizontal shaker for 90 min. The insoluble part was removed by ultracentrifugation for 30 min at 160 000*g*. Then, 10 mM $MgCl_2$ and 50 μg/mL of DNase (Roche) were added, and the solution was incubated with equilibrated Streptavidin UltraLink Resin (Pierce). After 90 min of agitation at 4 °C, the beads were washed three times with five bed volumes of 50 mM Na_2HPO_4, pH 7.5, 290 mM NaCl, 10 mM KCl, and 0.05% DDM. Finally, the protein was eluted in wash buffer containing 3 mM biotin and concentrated using a 100 kDA MWCO Amicon centrifugal filter (Millipore).

For size-exclusion chromatography, the concentrated protein was loaded on a Superose 6 10/300 GL column (GE Healthcare) equilibrated with wash buffer coupled to an Agilent 1200 HPLC system and run at 0.2 mL/min. UV absorbance and tryptophan fluorescence (280 nm excitation, 350 nm emission) were recorded and normalized. The following amounts of purified protein were injected on SEC: 81 μg of hERG-FL, 51 μg of hERGΔN, 25 μg of hERGΔNΔC, 67 μg of hERG KcsA, 66 μg of hERG GCN-LI, and 64−111 μg of hERG GCN-II, -IL, and-DD.

The yields of purified hERG constructs varied between 125 (hERGΔNΔC) and 380 μg (hERG KcsA and hERG GCN-LI) per liter of HEK cells.

Electrophysiology. The constructs in pTLN FX were linearized with MluI and transcribed into capped complementary RNA with the mMessage mMachine SP6 kit (Ambion). The RNA was purified with High Pure RNA isolation kit (Roche), and 5 ng of RNA was injected per defolliculated oocyte. Oocytes were maintained in Barth's solution containing 1 mM sodium pyruvate and 50 mg/L of gentamycine for 3 days at 16 °C. Then, they were measured on a two-electrode voltage-clamp setup (OC-725B, Warner) at 20 °C. Currents were recorded in bath solutions containing 5 mM HEPES, pH 7.4, 94 mM NaCl, 4 mM KCl, 1 mM $MgCl_2$, and 0.3 mM $CaCl_2$.

Digitized data were analyzed with Clampfit (Molecular Devices) and GraphPad software.

To assess the activation of the chimeric channels, the transmembrane voltage of injected oocytes was stepped from a holding potential of −80 mV to activation voltages ranging from −70 to +40 mV in 10 mV increments for 4 s and then back to −50 mV for 2s.

For inhibition, oocytes were depolarized to +20 mV with a 2 s pulse from a holding potential of −80 mV and then repolarized to −40 mV for 1.5 s to record the tail currents. This protocol was repeated every 10 s.

Oocytes were superfused with bath solution containing astemizole for 10 min to reach a binding equilibrium while recording the inhibition protocol. For BeKm-1, it was sufficient to superfuse for 3 min.

Introduction of an Extracellular HA Tag. A HA epitope tag was introduced between T443 and E444 in the extracellular S1/S2 loop with overlap-extension PCR according to Ficker et al.[30] However, the inserted sequence was changed from NSEHYPYDVPDYAVTFE to NGGHYPYDVPDYAVGGE.

The inserted tag did not affect the electrophysiological properties of the channel.

Single-Cell ELISA. Three days after RNA injection, *X. laevis* oocytes were assayed with single-cell ELISA. Surface labeling of oocytes was performed according to Zerangue et al.[31] The antibodies used were anti-HA high affinity (3F10, Roche) and HRP-conjugated donkey anti-rat F(ab′)$_2$ fragments (Jackson Immuno Research). Oocytes were injected with RNA coding for the HA-tagged constructs and placed in a 96-well plate with Barth's solution on a 1% agarose cushion. All labeling and washing steps were performed in this plate. Finally, single oocytes were transferred into the agarose-cushioned wells of a white flat-bottomed plate filled with ND96 solution. Before the measurement, the solution was aspirated and 30 μL of Super Signal ELISA femto (Pierce) solutions 1 and 2 was added. After mixing, the plate was measured in luminescence mode with an Infinite M1000 plate reader (Tecan).

Western Blot. Oocyte membranes were prepared according to Tucker et al.[32] Membranes corresponding to four oocytes were resolved by 5−20% SDS-PAGE and then transferred onto a nitrocellulose membrane and blocked with 1% western blocking reagent (Roche). The membrane was incubated with anti-HA high affinity antibody followed by HRP-conjugated donkey anti-rat F(ab′)$_2$ fragment and developed with Super Signal West Pico Chemiluminescent Substrate (Pierce).

RESULTS AND DISCUSSION

Purification of hERG Full-Length Results in hERG Monomers. Expression and purification of hERG full length (FL) is extremely difficult. Zhang et al. were unable to solubilize hERG-FL His expressed in Sf9 insect cells with DDM.[33] We also attempted to produce detergent-solubilized hERG-FL His expressed in Sf9 insect cells and were only able to solubilize the protein in harsh detergents, resulting in monomeric channels. In contrast to insect cells, hERG-FL produced in a commercial HEK cell line could be extracted with DDM. Despite this mild detergent extraction, the tetrameric channel dissociated.[32] For reference purposes we again prepared monomeric hERG-FL from HEK cells (Figure S1). In addition, we screened for constructs that are stable as tetrameric channels in detergent solution and retain the channel properties in electrophysiological experiments.

Construction of Chimeric hERG Channels. To find the minimal functional unit of the hERG channel and to gain insight into the roles of the cytoplasmic domains in gating, we deleted either the PAS domain and the distal C-terminus or the PAS domain and the C-linker/CNBD including the distal C-terminus, yielding hERGΔN (362−870) and hERGΔNΔC (362−669) (Figure 1A). The N-terminal amino acid sequence KIKER that was shown to influence the activation gating was still present in these constructs.[33]

Because of the low detergent stability of hERG-FL, we decided to promote the tetrameric association of hERG by substitution of the inherent tetramerization domain C-linker/

dx.doi.org/10.1021/bi401100a | *Biochemistry* 2013, 52, 9237−9245

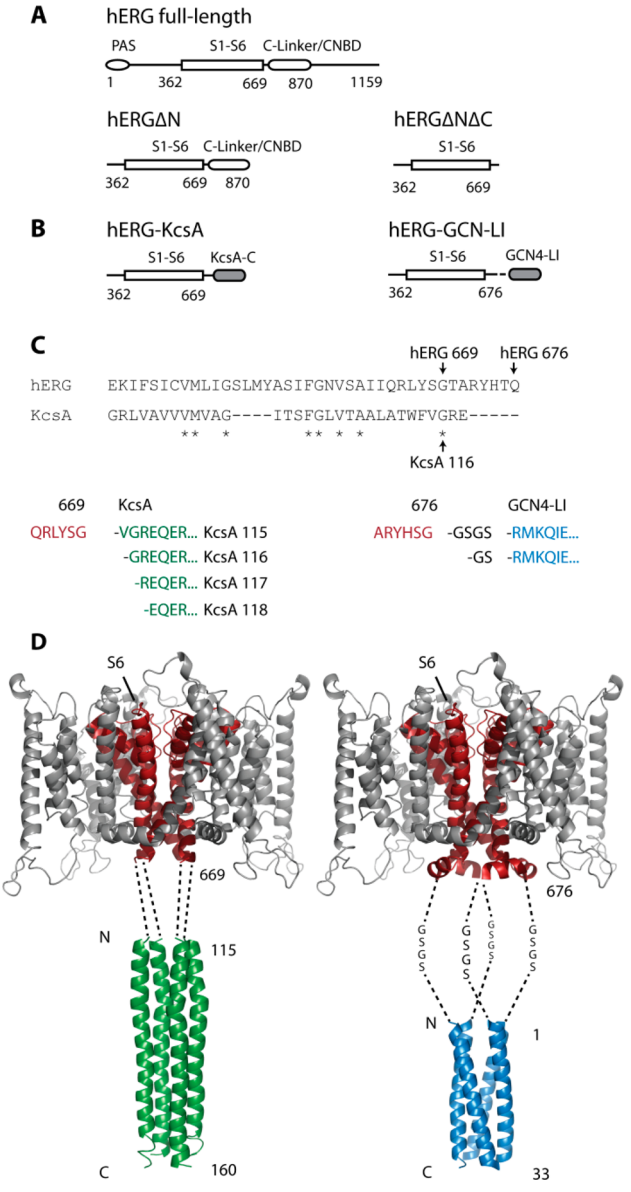

Figure 1. Overview of the hERG truncations and considerations for the construction of chimeric channels. (A) Schematics of hERG-FL and two truncations used in this study. The S1−S6 domain encompasses the six transmembrane helices plus the pore helix of hERG. (B) Chimeric channels hERG-KcsA and hERG-GCN-LI were produced by fusing either the C-terminus of KcsA or the GCN4-LI leucine zipper to hERGΔNΔC, respectively. (C) Sequence alignment of hERG residues 637−676 and KcsA residues 88−118. The sequences at the bottom indicate the residues of hERG-KcsA and -GCN-LI that were connected. The numbers identify the end position of hERG. hERG-KcsA 115 contains a fragment of the KcsA C-terminal helix ranging from residues 115 to 160, hERG-KcsA 116, from 116 to 160, hERG-KcsA 117, from 117 to 160, and hERG-KcsA 118, from 118 to 160. hERG-GCN-LI contains an additional -GS- or -GSGS- linker. (D) Structural considerations for the generation of chimeric hERG channels. Residues 409−669 (left) and 409−676 (right) from the homology model of hERG are displayed. Residues 612−669 and 612−676 are highlighted in red; this part encompasses the pore helix and the S6 helix as well as the first helix of the C-linker for hERG-GCN-LI. The crystal structures of KcsA-FL residues 115−160 (PDB: 3EFF) and the GCN4-LI (PDB: 1GCL) coiled coil are colored green and blue, respectively.

CNBD either with the cytoplasmic C-terminal KcsA helix or with the GCN4-LI leucine zipper.

First, we built a homology model of hERG to guide our decisions on how to attach the artificial tetramerization domains. We chose two different hERG end positions, one on the cytoplasmic side of the S6 transmembrane helix and one in the middle of the first C-linker helix (Figure 1B). Both fragments retained the residues in the S6 helix that were shown to be crucial for activation gating.[34] For the construction of the hERG-KcsA chimera, we grafted the KcsA helix with different start positions directly to the C-terminus of hERGΔNΔC at position 669. A sequence alignment of the S6 helices from hERG and KcsA revealed that hERG G669 overlaps with KcsA G116 (Figure 1C). Therefore, KcsA start positions were chosen ranging from residues 115 to 118 to cover more than one helical turn and multiple orientations of the tetramer-forming helices. GCN4-LI was prepared by linking GCN4-LI to hERGΔNΔC at position 676 using a -GS- or -GSGS- linker. Obviously, the orientation of the cytosolic tetramerization domains relative to the channel core is critical and must be precisely mimicked by the hybrid molecules. A hypothetical structural arrangement of the chimeric channels is displayed in Figure 1D.

Tetramerization is Critical for hERG Function. To study the activation gating, we probed the hERG truncations and chimeric channels with a voltage-pulse protocol to elicit a family of outward currents in *X. laevis* oocytes. The channels were activated with a series of voltage pulses from −70 to +40 mV in 10 mV increments. Then, the voltage was stepped back to −50 mV.

hERGΔN produced functional channels in electrophysiological recordings, whereas the deletion of the C-linker/CNBD in hERGΔNΔC abolished channel function (Figure 2B,C). The C-linker/CNBD was reported to be essential for channel function, as deletion of these domains abolished the channel activity and cell surface expression.[35] For the chimeric hERG-KcsA channel, four constructs with KcsA start positions 115, 116, 117, and 118 were tested (Figure 1B). In general, the addition of the KcsA helix to hERGΔNΔC restored the voltage-dependent gating properties of the channel. hERG-KcsA 115, starting at position 115, was used for further experiments because it produced the highest currents in the two-electrode voltage-clamp recording that most closely resembled the hERG-FL recordings (Figure 2A,D−G). The fusion of KcsA at position 117 (Figure 2F) led to the formation of a channel without hERG features. For hERG-GCN4-LI, two constructs with different linker lengths between hERGΔNΔC and GCN4-LI were tested (Figure 1C). The longer linker produced more pronounced currents in two-electrode voltage-clamp recordings and was thus chosen for further experiments (Figure 2H). These findings underscore the importance of a precise arrangement of the tetramerization domains to produce functional chimeric channels.

Using the approach with chimeric channels, we generated the shortest functional hERG construct described so far.

General Gating Behavior of the hERG Constructs. The maximal outward current at the end of each depolarization step was used to construct the current−voltage (I−V) relationship. The I−V plot demonstrated that the inactivation in the chimeric channels was still intact and that the maxima were slightly left-shifted in relation to hERG-FL. In contrast, hERGΔN displayed a significant right shift of more than 30 mV (Figure 3A).

dx.doi.org/10.1021/bi401100a | *Biochemistry* 2013, 52, 9237−9245

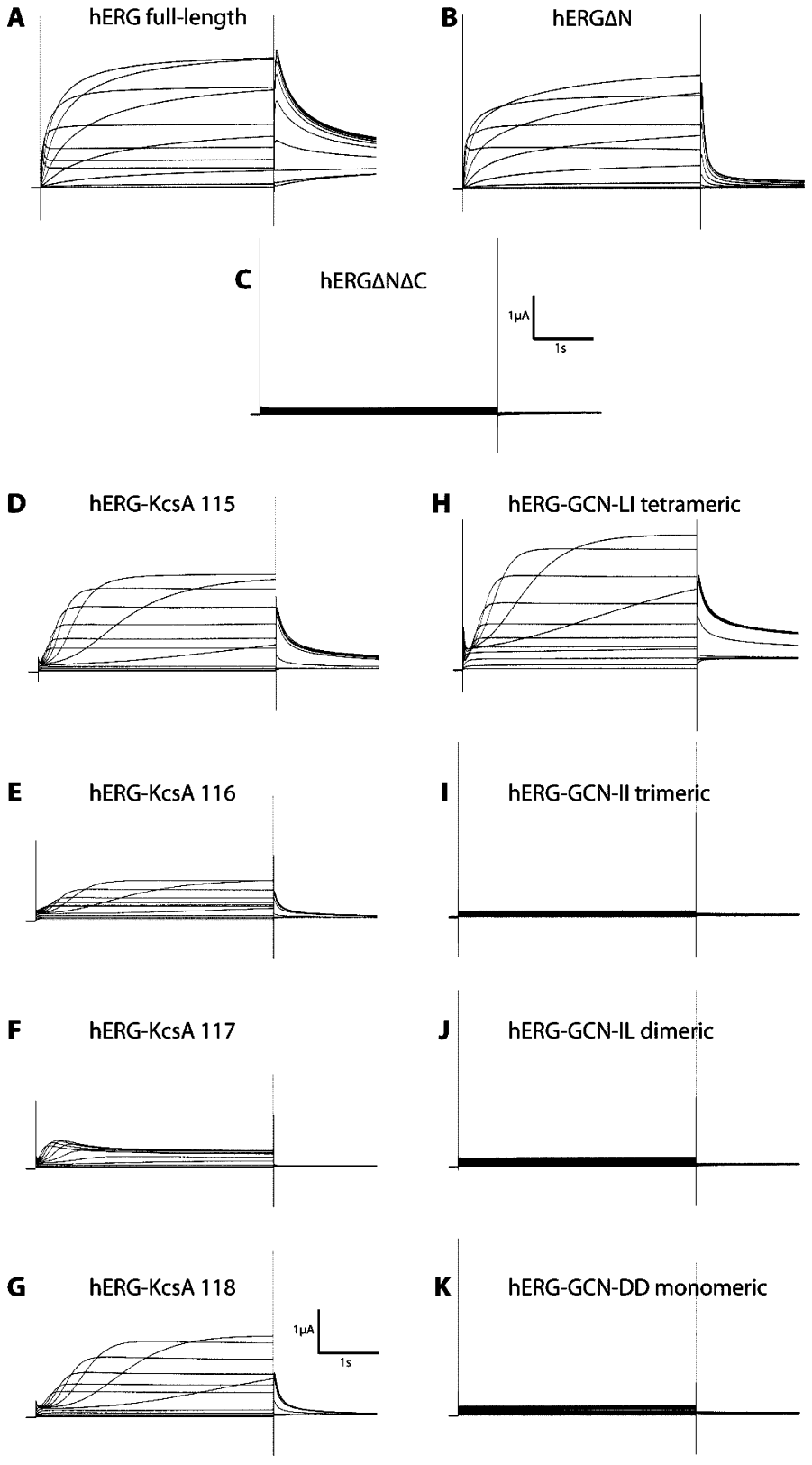

Figure 2. Function of hERGΔNΔC is rescued with the addition of a tetramerization domain. Wild-type hERG (A), hERG truncations (B, C), and chimeric hERG channels (D−K) are displayed. Steady-state activation currents in *Xenopus* oocytes were evoked with the activation voltage protocol described in the Experimental Procedures. All traces were scaled identically; the scale bars correspond to 1 μA and 1s, respectively.

The steady-state voltage dependence of activation relationship ($G-V$) was obtained by plotting the peak tail current versus the activation voltage. The Boltzmann fit of the $G-V$ data revealed a right shift of the voltage for half-maximal activation ($V_{1/2}$) for hERGΔN relative to hERG-FL. This shift was explained with the deletion of the proximal N-terminal

dx.doi.org/10.1021/bi401100a | *Biochemistry* 2013, 52, 9237−9245

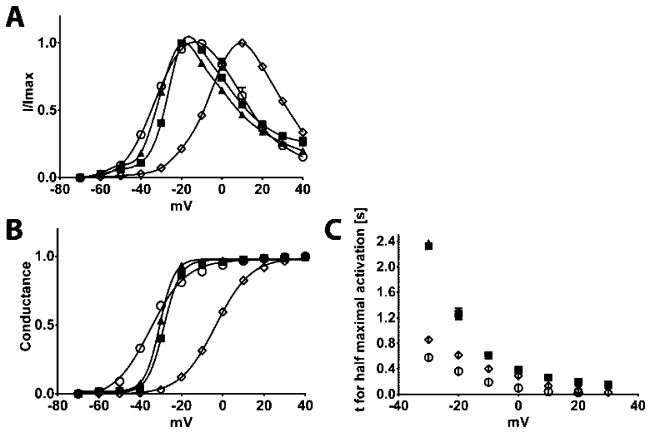

Figure 3. (A) Current–voltage relationship for hERG WT (○), hERGΔN (◊), hERG-KcsA 115 (■), and hERG GCN-LI (▲). Currents at the end of a 4 s activating pulse were normalized to the maximal current at the end of the pulse ($n \geq 4$). (B) Steady-state voltage-dependence of activation (G–V). The tail currents at −50 mV were normalized to the peak tail current, plotted against the voltage, and fitted with a Boltzmann function to estimate the half point ($V_{1/2}$) and k value (slope) ($n = 5$). hERG WT (○) ($V_{1/2} = -35$ mV ± 0.4 mV, $k = 8.7 \pm 0.4$ mV), hERG ΔN (◊) ($V_{1/2} = -3.5$ mV ± 0.2 mV, $k = 8.5 \pm 0.2$ mV), hERG-KcsA 115 (■) ($V_{1/2} = -28.4 \pm 0.2$ mV, $k = 4 \pm 0.2$ mV), and hERG GCN-LI (▲) ($V_{1/2} = -30.5$ mV ± 0.2 mV, $k = 3.6 \pm 0.2$ mV). (C) Time to reach half-maximal activation versus voltage ($n = 3$). The time after the depolarizing step at which the current reached half of its maximal value was determined manually. hERG-KcsA 115 and hERG-GCN-LI display identical activation kinetics. Values are represented as the mean ± SEM.

domain.[17,36] The right shift of $V_{1/2}$ was far less pronounced for the chimeric channels, but their k (slope) value was more than 2-fold lower (Figure 3B).

Kinetic Determinants of Deactivation and Activation Gating. When comparing tail currents in Figure 2, it is conspicuous that deactivation in hERGΔN (Figure 2B) occurs much faster than in hERG-FL (Figure 2A), which was explained with the deletion of the PAS domain.[15,37,38] However, hERG-KcsA 115 and hERG-GCN-LI exhibited a slow deactivation as well, although they were missing the PAS domain. Their slow deactivation closely matched the one from the hERG-FL channel.

Channel deactivation is influenced by the interplay between the N-terminal PAS domain and the C-terminal CNBD.[17,36] Even though both chimeric channels lack the PAS domain as well as the C-linker/CNBD, they had slower deactivation kinetics than hERGΔN. Therefore, this effect originates solely from the insertion of an artificial tetramerization domain. These results point to an open state that is more stable in the chimeric channels and resembles the behavior of hERG-FL.

Next, we analyzed the channel activation kinetics. hERG-KcsA 115 and hERG-GCN-LI had an up to 3-fold increased time to reach half-maximal activation at voltages below 0 mV (Figure 3C) compared to hERG-FL. Interestingly, hERG-KcsA 115 and hERG-GCN-LI had identical kinetic properties and very similar gating characteristics, although they have different fusion sites and tetramerization domains. Gustina et al. demonstrated that a deletion of the CNBD (amino acids 749–872) reduced the timespan of activation up to 3-fold relative to hERG-FL.[17]

Astemizole and BeKm-1 Block the Chimeric Channels. We used the potent hERG inhibitor astemizole to determine if the fusion of the two artificial tetramerization domains to hERGΔNΔC distorted the orientation of the pore-lining residues, which are responsible for drug interaction.[39–42] It was shown that the residues F656 and Y652 located in the S6 helix point into the hERG channel pore and form an aromatic ring where most of the inhibitors bind. Chen et al. found a more than 10-fold decreased affinity for cisapride for a hERG mutant that had phenylalanine residue 656 shifted to position 655, whereas shifting it to 657 removed most of the cisapride block.[41] If the mutual orientation of the drug binding residues in the S6 helix of the chimeric channels is altered, then the drug block would be greatly diminished.

Astemizole blocked hERG-FL in a concentration-dependent manner with an IC_{50} value of 15.8 ± 1.5 nM (Figure 4A). The

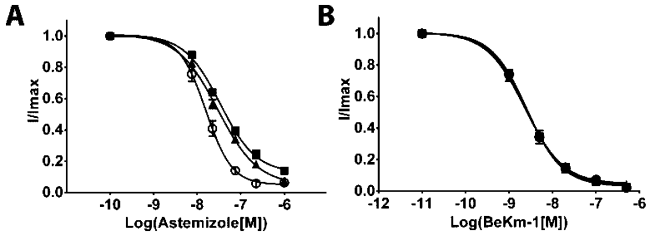

Figure 4. Pharmacological properties of chimeric channels. (A) Inhibition of hERG WT (○) hERG-KcsA 115 (■) and hERG GCN-LI (▲) tail currents by 7.5, 22.5, 75, and 225 nM and 1 μM astemizole ($n = 4$). (B) Inhibition of tail currents by 1, 5, 20, 100, and 500 nM BeKm-1 ($n = 3$). Tail currents were measured at −40 mV after a 2 s depolarization step to +20 mV. Values are represented as the mean ± SEM.

IC_{50} for hERG-KcsA 115 and hERG-GCN-LI were 33.8 ± 3.2 and 29.8 ± 3.5 nM, respectively. Our IC_{50} values for the inhibition of the channel by astemizole were about 2-fold higher for the chimeric channels than for hERG-FL. Thus, the position of residues F656 and Y652 seems to differ slightly between hERG-FL and the chimeric channels. Still, these residues are close enough to the original orientation to allow the interaction with astemizole.

The hERG-specific toxin BeKm-1 was used to test the integrity of the S5–P linker and P loop region in the chimeric hERG channels.[43] The dose–response curves of hERG-FL, hERG-KcsA 115, and hERG-GCN-LI (Figure 4B) were basically indistinguishable. The IC_{50} values for the BeKm-1 block of hERG-FL, hERG-KcsA 115, and hERG-GCN-LI were 2.5 ± 0.3, 2.6 ± 0.1, and 2.3 ± 0.2 nM respectively. These IC_{50} values indicate an unaltered outer mouth structure of the chimeric channels compared to hERG-FL.

Trafficking in *Xenopus laevis* Oocytes. We analyzed the trafficking and expression in oocytes to elucidate why the hERGΔNΔC construct produced no currents in two-electrode voltage-clamp recordings.

To compare the cell surface expression of the constructs, we introduced a hemagglutinin (HA) epitope into the extracellular loop between S1 and S2.[30] Then, we performed single-cell ELISA on oocytes to quantify the relative amounts of hERG-HA that reached the cell membrane (Figure 5A). hERG-FL and hERGΔN reached the membrane, but hERGΔNΔC membrane levels were 14-fold decreased relative to hERG-FL. This explained the inability of this construct to form intact channels in two-electrode voltage-clamp recordings. Fusion of the C-terminal helix of KcsA or GCN-LI to hERGΔNΔC rescued the surface expression as well as the channel function.

dx.doi.org/10.1021/bi401100a | *Biochemistry* 2013, 52, 9237–9245

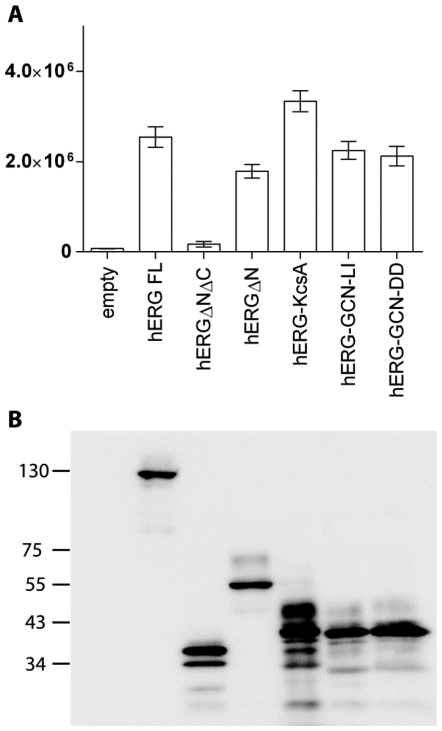

Figure 5. Trafficking of chimeric hERG channels. (A) Surface expression of HA-tagged hERG constructs in *Xenopus* oocytes quantified with single-cell ELISA. Bars represent the mean relative light units ± SEM from 11 oocytes per construct. (B) Western blot of total HA-tagged proteins from oocyte lysates. The amount of protein corresponding to four oocytes was loaded per lane and blotted with anti-HA antibody. Degradation products are visible for hERG-KcsA and hERGΔNΔC.

Western blot analysis of oocyte membrane fractions showed that hERGΔNΔC was expressed at similar levels as the other constructs (Figure 5B). Therefore, the trafficking from the ER to the plasma membrane was impaired for hERGΔNΔC.

To assess if the forward trafficking from the ER to the plasma membrane of requires hERG to be tetrameric, we used hERG-GCN-DD, which contains a monomeric version of the coiled coil.[23] This construct was unable to form functional channels, as judged by two-electrode voltage-clamp recordings, but it was expressed to a similar extent as hERG-GCN-LI and reached the cell surface as well, as judged by cell surface ELISA data (Figure 5A). The trimeric hERG-GCN-II behaved identically (data not shown). These data suggest that the ER and Golgi export of hERG does not require the channel to be tetrameric. One explanation could be that the additional domain masked an otherwise exposed ER or Golgi retention signal.[44]

A hint for a similar retention of hERGΔNΔC in HEK cells arose from the different glycosylation pattern of purified hERG-FL, hERGΔNΔC, hERGΔN, and hERG-KcsA 115. The hERG trafficking status in mammalian cells is inferred from the presence of a glycosylation band.[45] The core glycosylated form is produced in the ER, and another more complex glycosylation is attached in the Golgi compartments. hERGΔNΔC expressed in HEK cells was missing a higher molecular weight band originating from glycosylation (Figure S2), indicating that the trafficking of this construct in mammalian cells stalls at an early stage. Therefore, the single-cell ELISA results from oocytes are most likely transferable to mammalian cells.

Oligomerization Domains of GCN4 and KcsA Dictate the Oligomeric State of the Purified Chimeric Channels. We attempted to verify the tetramerization of the purified chimeric channels in vitro. For this, we expressed the hERG truncations and the chimeric channels in HEK cells and purified them in detergent solution. To assess the oligomeric state, we analyzed the purified proteins by size-exclusion chromatography. hERGΔN and hERGΔNΔC eluted at 15.6 and 16 mL, respectively, on a Superose 6 column, whereas the chimeric channels hERG-KcsA 115 and hERG-GCN-LI eluted at 13.7 and 13.9 mL, respectively, which corresponds to an apparent molecular weight of a tetrameric protein (Figure 6A). The elution volumes of hERGΔN and hERGΔNΔC indicated that the channels dissociated into their subunits when they were solubilized with detergent.

It was possible to disassemble the hERG-KcsA 115 oligomer by exchanging the detergent for purification. When DDM was replaced by with the harsher zwitterionic detergent Fos-Choline-12, hERG-KcsA 115 eluted at a similar retention

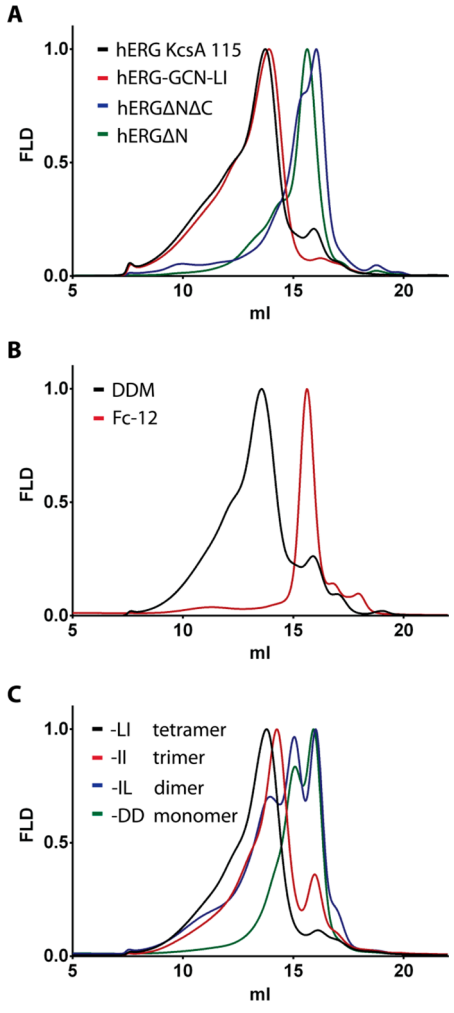

Figure 6. (A) Size-exclusion chromatograms of purified hERG truncations and chimeric hERG channels on a Superose 6 column. (B) Elution profiles of hERG-KcsA 115 solubilized and purified either in DDM or Fos-Choline-12. (C) Calibration of the column with different oligomeric species of the purified hERG-GCN4 chimera. Isolated GCN4-DD, -IL, II, and LI form monomers, dimers, trimers, and tetramers in solution, respectively. The chimeric hERG-GCN4 versions show a similar behavior.

dx.doi.org/10.1021/bi401100a | *Biochemistry* 2013, 52, 9237−9245

volume as observed for hERGΔNΔC (Figure 6B). hERGΔNΔC had an identical elution volume in DDM and Fos-Choline-12 detergent (data not shown), pointing to the appearance of a monomeric form in both detergents.

To determine the oligomeric state of the purified channels, we calibrated the SEC column with different oligomeric forms of hERG-GCN. We introduced mutations in the GCN-LI part of the hERG-GCN-LI chimera to obtain trimeric (GCN-II), dimeric (GCN-IL), and monomeric (GCN-DD) versions of the coiled coil.[23,24] The purified hERG-GCN-LI, hERG-GCN-II, hERG-GCN-IL, and hERG-GCN-DD eluted at increasing elution volumes (Figure 6C). The dimeric hERG-GCN-IL displayed three peaks, where the middle one probably reflects the dimeric version. The monomeric hERG-GCN-DD had an additional dimeric peak in front. However, the elution volume of the main peak of hERG-GCN-DD corresponded to the hERGΔNΔC as well as the disassembled hERG-KcsA 115. These results suggest that the chimeric channels hERG-KcsA 115 and hERG-GCN-LI retain their tetrameric assembly during purification.

Two-electrode voltage-clamp recordings of hERG-GCN-LI, hERG-GCN-II, hERG-GCN-IL, and hERG-GCN-DD revealed that only the tetrameric version hERG-GCN-LI formed functional channels (Figure 2H–K).

The replacement of the inherent tetramerization domains with stable coiled coils increased the oligomeric stability of a minimal hERG construct and enabled the chimeric channels to keep their tetrameric state during solubilization and purification. The results obtained from various constructs highlight the importance of the connection between the membrane part and the tetramerization domains, which is critical for the channel function in chimeric and native hERG channels.

We conclude that the gating characteristics of chimeric hERG channels are very close to the hERG-FL channel and that they share the inhibition by BeKm-1 and astemizole. In addition, the generation of chimeric hERG channels enabled deeper insight into the kinetic determinants of activation and deactivation gating. The tetramerization is required for the voltage-dependent gating function of hERG but not for its correct trafficking in *X. laevis* oocytes. This requirement could be correlated with the tetrameric assembly of purified chimeric channels observed in SEC.

The availability of purified and functional chimeric hERG provides new opportunities for functional, biochemical, and structural studies that will help to understand the mechanism of drug binding and LQTS.

■ ASSOCIATED CONTENT

Supporting Information

SEC analysis of hERG-FL, SDS-PAGE gels of purified constructs, and response of purified chimeric channels to pH changes. This material is available free of charge via the Internet at http://pubs.acs.org.

■ AUTHOR INFORMATION

Corresponding Author

*E-mail: gruetter@bioc.uzh.ch; Tel: +41446355580.

Author Contributions

The manuscript was written through contributions of all authors. All authors have given approval to the final version of the manuscript.

Funding

This work was supported by the University of Zürich within the framework of the Swiss NCCR Structural Biology program and the Swiss Commission of Technology and Innovation (CTI). G.J.H. is affiliated with the Ph.D. program in Biomolecular Structure and Mechanism of the Life Science Zürich Graduate School.

Notes

The authors declare no competing financial interest.

■ ACKNOWLEDGMENTS

We thank Prof. Raimund Dutzler for introducing us to electrophysiology and for helpful discussions. We thank Dr. Thomas Heitkamp for support during the project and Dr. Christophe Briand for the generation of the hERG homology model. We are grateful to Bernhard Gsell for providing the purified toxin BeKm-1. We thank Dr. Iwan Zimmermann and Carlo Bertozzi for the donation of the pTLN Fx vector and for help with two-electrode voltage-clamp recordings. We thank Dr. Stefan Schenk for the kind donation of the pcDNA 3.1-SBP Fx vector and for help with expression in HEK cells.

■ ABBREVIATIONS USED

hERG, human *ether-a-go-go-related gene*; DDM, *n*-dodecyl-*β*-D-maltopyranoside; SEC, size-exclusion chromatography

■ REFERENCES

(1) Bianchi, L., Wible, B., Arcangeli, A., Taglialatela, M., Morra, F., Castaldo, P., Crociani, O., Rosati, B., Faravelli, L., Olivotto, M., and Wanke, E. (1998) *herg* encodes a K^+ current highly conserved in tumors of different histogenesis: A selective advantage for cancer cells? *Cancer Res. 58*, 815–822.

(2) Sanguinetti, M. C., Jiang, C., Curran, M. E., and Keating, M. T. (1995) A mechanistic link between an inherited and an acquired cardiac arrhythmia: HERG encodes the I_{Kr} potassium channel. *Cell 81*, 299–307.

(3) Furlan, F., Taccola, G., Grandolfo, M., Guasti, L., Arcangeli, A., Nistri, A., and Ballerini, L. (2007) ERG conductance expression modulates the excitability of ventral horn GABAergic interneurons that control rhythmic oscillations in the developing mouse spinal cord. *J. Neurosci. 27*, 919–928.

(4) Sanguinetti, M. C., and Jurkiewicz, N. K. (1991) Delayed rectifier outward K^+ current is composed of two currents in guinea pig atrial cells. *Am. J. Physiol. 260*, H393–H399.

(5) Wang, D. T., Hill, A. P., Mann, S. A., Tan, P. S., and Vandenberg, J. I. (2011) Mapping the sequence of conformational changes underlying selectivity filter gating in the K(v)11.1 potassium channel. *Nat. Struct. Mol. Biol. 18*, 35–41.

(6) Snyders, D. J., and Chaudhary, A. (1996) High affinity open channel block by dofetilide of HERG expressed in a human cell line. *Mol. Pharmacol. 49*, 949–955.

(7) Trudeau, M. C., Warmke, J. W., Ganetzky, B., and Robertson, G. A. (1995) HERG, a human inward rectifier in the voltage-gated potassium channel family. *Science 269*, 92–95.

(8) Curran, M. E., Splawski, I., Timothy, K. W., Vincent, G. M., Green, E. D., and Keating, M. T. (1995) A molecular basis for cardiac arrhythmia: HERG mutations cause long QT syndrome. *Cell 80*, 795–803.

(9) Hancox, J. C., McPate, M. J., El Harchi, A., and Zhang, Y. H. (2008) The hERG potassium channel and hERG screening for drug-induced torsades de pointes. *Pharmacol. Ther. 119*, 118–132.

(10) Anderson, C. L., Delisle, B. P., Anson, B. D., Kilby, J. A., Will, M. L., Tester, D. J., Gong, Q., Zhou, Z., Ackerman, M. J., and January, C. T. (2006) Most LQT2 mutations reduce Kv11.1 (hERG) current by a class 2 (trafficking-deficient) mechanism. *Circulation 113*, 365–373.

(11) Ficker, E., Thomas, D., Viswanathan, P. C., Dennis, A. T., Priori, S. G., Napolitano, C., Memmi, M., Wible, B. A., Kaufman, E. S., Iyengar, S., Schwartz, P. J., Rudy, Y., and Brown, A. M. (2000) Novel characteristics of a misprocessed mutant HERG channel linked to hereditary long QT syndrome. *Am. J. Physiol.: Heart Circ. Physiol. 279*, H1748−1756.
(12) Wang, Y., Huang, X., Zhou, J., Yang, X., Li, D., Mao, H., Sun, H. H., Liu, N., and Lian, J. (2012) Trafficking-deficient G572R-hERG and E637K-hERG activate stress and clearance pathways in endoplasmic reticulum. *PLoS One 7*, e29885-1−e29885-7.
(13) Hille, B. (1992) *Ionic Channels of Excitable Membranes*, Sinauer Associates Inc., Sunderland, MA.
(14) Fernandez, D., Ghanta, A., Kauffman, G. W., and Sanguinetti, M. C. (2004) Physicochemical features of the HERG channel drug binding site. *J. Biol. Chem. 279*, 10120−10127.
(15) Schönherr, R., and Heinemann, S. H. (1996) Molecular determinants for activation and inactivation of HERG, a human inward rectifier potassium channel. *J. Physiol. 493*, 635−642.
(16) Fernandez-Trillo, J., Barros, F., Machin, A., Carretero, L., Dominguez, P., and de la Pena, P. (2011) Molecular determinants of interactions between the N-terminal domain and the transmembrane core that modulate hERG K^+ channel gating. *PLoS One 6*, e24674-1−e24674-12.
(17) Gustina, A. S., and Trudeau, M. C. (2011) hERG potassium channel gating is mediated by N- and C-terminal region interactions. *J. Gen. Physiol. 137*, 315−325.
(18) Akhavan, A., Atanasiu, R., Noguchi, T., Han, W., Holder, N., and Shrier, A. (2005) Identification of the cyclic-nucleotide-binding domain as a conserved determinant of ion-channel cell-surface localization. *J. Cell Sci. 118*, 2803−2812.
(19) Kupershmidt, S., Snyders, D. J., Raes, A., and Roden, D. M. (1998) A K^+ channel splice variant common in human heart lacks a C-terminal domain required for expression of rapidly activating delayed rectifier current. *J. Biol. Chem. 273*, 27231−27235.
(20) Brelidze, T. I., Gianulis, E. C., Dimaio, F., Trudeau, M. C., and Zagotta, W. N. (2013) Structure of the C-terminal region of an ERG channel and functional implications. *Proc. Natl. Acad. Sci. U.S.A. 110*, 11648−11653.
(21) Brelidze, T. I., Carlson, A. E., Sankaran, B., and Zagotta, W. N. (2012) Structure of the carboxy-terminal region of a KCNH channel. *Nature 481*, 530−533.
(22) Molina, M. L., Encinar, J. A., Barrera, F. N., Fernández-Ballester, G., Riquelme, G., and González-Ros, J. M. (2004) Influence of C-terminal protein domains and protein-lipid interactions on tetramerization and stability of the potassium channel KcsA. *Biochemistry 43*, 14924−14931.
(23) Zerangue, N., Jan, Y. N., and Jan, L. Y. (2000) An artificial tetramerization domain restores efficient assembly of functional Shaker channels lacking T1. *Proc. Natl. Acad. Sci. U.S.A. 97*, 3591−3595.
(24) Harbury, P. B., Zhang, T., Kim, P. S., and Alber, T. (1993) A switch between two-, three-, and four-stranded coiled coils in GCN4 leucine zipper mutants. *Science 262*, 1401−1407.
(25) Geertsma, E. R., and Dutzler, R. (2011) A versatile and efficient high-throughput cloning tool for structural biology. *Biochemistry 50*, 3272−3278.
(26) Lorenz, C., Pusch, M., and Jentsch, T. J. (1996) Heteromultimeric CLC chloride channels with novel properties. *Proc. Natl. Acad. Sci. U.S.A. 93*, 13362−13366.
(27) Keefe, A. D., Wilson, D. S., Seelig, B., and Szostak, J. W. (2001) One-step purification of recombinant proteins using a nanomolar-affinity streptavidin-binding peptide, the SBP-Tag. *Protein Expression Purif. 23*, 440−446.
(28) Kelley, L. A., and Sternberg, M. J. E. (2009) Protein structure prediction on the Web: A case study using the Phyre server. *Nat. Protoc. 4*, 363−371.
(29) Chen, C., and Okayama, H. (1987) High-efficiency transformation of mammalian cells by plasmid DNA. *Mol. Cell. Biol. 7*, 2745−2752.
(30) Ficker, E., Dennis, A. T., Wang, L., and Brown, A. M. (2003) Role of the cytosolic chaperones Hsp70 and Hsp90 in maturation of the cardiac potassium channel HERG. *Circ. Res. 92*, e87−100.
(31) Zerangue, N., Schwappach, B., Jan, Y. N., and Jan, L. Y. (1999) A new ER trafficking signal regulates the subunit stoichiometry of plasma membrane K(ATP) channels. *Neuron 22*, 537−548.
(32) Tucker, S. J., Bond, C. T., Herson, P., Pessia, M., and Adelman, J. P. (1996) Inhibitory interactions between two inward rectifier K^+ channel subunits mediated by the transmembrane domains. *J. Biol. Chem. 271*, 5866−5870.
(33) Saenen, J. B., Labro, A. J., Raes, A., and Snyders, D. J. (2006) Modulation of HERG gating by a charge cluster in the N-terminal proximal domain. *Biophys. J. 91*, 4381−4391.
(34) Wynia-Smith, S. L., Gillian-Daniel, A. L., Satyshur, K. A., and Robertson, G. A. (2008) hERG gating microdomains defined by S6 mutagenesis and molecular modeling. *J. Gen. Physiol. 132*, 507−520.
(35) Aydar, E., and Palmer, C. (2001) Functional characterization of the C-terminus of the human ether-à-go-go-related gene K(+) channel (HERG). *J. Physiol. 534*, 1−14.
(36) Gustina, A. S., and Trudeau, M. C. (2013) The eag domain regulates hERG channel inactivation gating via a direct interaction. *J. Gen. Physiol. 141*, 229−241.
(37) Morais Cabral, J. H., Lee, A., Cohen, S. L., Chait, B. T., Li, M., and Mackinnon, R. (1998) Crystal structure and functional analysis of the HERG potassium channel N terminus: A eukaryotic PAS domain. *Cell 95*, 649−655.
(38) Spector, P. S., Curran, M. E., Keating, M. T., and Sanguinetti, M. C. (1996) Class III antiarrhythmic drugs block HERG, a human cardiac delayed rectifier K^+ channel. Open-channel block by methanesulfonanilides. *Circ. Res. 78*, 499−503.
(39) Chiu, P. J. S., Marcoe, K. F., Bounds, S. E., Lin, C.-H., Feng, J.-J., Lin, A., Cheng, F.-C., Crumb, W. J., and Mitchell, R. (2004) Validation of a [3H]astemizole binding assay in HEK293 cells expressing HERG K^+ channels. *J. Pharmacol. Sci. 95*, 311−319.
(40) Suessbrich, H., Waldegger, S., Lang, F., and Busch, A. E. (1996) Blockade of HERG channels expressed in Xenopus oocytes by the histamine receptor antagonists terfenadine and astemizole. *FEBS Lett. 385*, 77−80.
(41) Chen, J., Seebohm, G., and Sanguinetti, M. C. (2002) Position of aromatic residues in the S6 domain, not inactivation, dictates cisapride sensitivity of HERG and eag potassium channels. *Proc. Natl. Acad. Sci. U.S.A. 99*, 12461−12466.
(42) Taglialatela, M., Pannaccione, A., Castaldo, P., Giorgio, G., Zhou, Z., January, C. T., Genovese, A., Marone, G., and Annunziato, L. (1998) Molecular basis for the lack of HERG K^+ channel block-related cardiotoxicity by the H1 receptor blocker cetirizine compared with other second-generation antihistamines. *Mol. Pharmacol. 54*, 113−121.
(43) Zhang, M., Korolkova, Y. V., Liu, J., Jiang, M., Grishin, E. V., and Tseng, G.-N. (2003) BeKm-1 is a HERG-specific toxin that shares the structure with ChTx but the mechanism of action with ErgTx1. *Biophys. J. 84*, 3022−3036.
(44) Ma, D., Taneja, T. K., Hagen, B. M., Kim, B.-Y., Ortega, B., Lederer, W. J., and Welling, P. A. (2011) Golgi export of the Kir2.1 channel is driven by a trafficking signal located within its tertiary structure. *Cell 145*, 1102−1115.
(45) Zhou, Z., Gong, Q., Ye, B., Fan, Z., Makielski, J. C., Robertson, G. A., and January, C. T. (1998) Properties of HERG channels stably expressed in HEK 293 cells studied at physiological temperature. *Biophys. J. 74*, 230−241.